

Comparison of Ultrafast Photodetectors Based on N⁺GaAs and LT GaAs

M. BIAŁOUS, R. MOGILINSKI, M. WIERZBICKI*, K. ŚWITKOWSKI AND B. PURA

Faculty of Physics, Warsaw University of Technology, Koszykowa 75, 00-662 Warszawa, Poland

(Received March 13, 2009; in final form November 22, 2010)

We present investigation of a photodetector based on nitrogen-ion-implanted GaAs. Device photoresponse signal shows 1.15 ps FWHM (400 GHz, 3 dB bandwidth) with the voltage amplitude ≈ 1 mV, measured using a constructed electro-optic sampling setup with 80 fs width, 795 nm wavelength and laser pulses repetition rate of 80 MHz. Changes in the shape of electrical signal for different beam powers excitation and voltage biases have been demonstrated, compared with LT GaAs photodetector based on the same finger geometry. Using technique of X-ray diffraction and diffuse scattering analyses we have observed the decrease of lattice constant, radius of nanoclusters after implantation, respectively, and linear density dislocations increased over twice.

PACS: 78.20.-e, 78.47.J-, 78.70.Ck

1. Introduction

In recent times ion-implanted-materials have been proposed as an alternative to low-temperature GaAs (LT GaAs) for construction of ultrafast photodetectors [1–3]. In this paper we investigate nitrogen implanted GaAs (N⁺GaAs) photodetector and compare it to LT GaAs based one. Ion implantation yields large concentration of arsenic antisite defects. These defects exhibit ellipsoidal or near-spherical form [4], conglomerated as nanometer clusters. X-ray diffraction curves present two distinguished regions corresponding to different distances from the defect core in ordinary space and different scattering intensities [5]. The first (Stokes–Wilson) region, closer to the defect core, contains crystal distortions. In the second (Huang) region — far from the defect, where crystal lattice distortions are weak — the symmetrical part of diffuse scattered intensity can be expressed as $I^s(q_0) \sim A \ln(e^{1/2}/q_0 R_0)$, where A involves the size and number of clusters as well as the wavelength of the radiation, R_0 is the mean cluster radius and $q_0 = |\mathbf{h}| \Delta\theta \cos\theta_B$, where \mathbf{h} is the reciprocal lattice diffraction vector, $\Delta\theta$ is the deviation from θ_B Bragg angle, e is Euler's constant.

For N⁺GaAs it is possible to obtain carrier lifetimes of only 100 fs [6]. This value is almost half shorter than for LT GaAs. After high temperature annealing ion implanted GaAs becomes a highly resistive material [7]. Implantation reduces both mobility and carrier concentration. N⁺GaAs exhibits sensitivity more than twice higher, and dark current orders of magnitude lower, com-

pared to that of LT GaAs. The sensitivity of N⁺GaAs is proportional to the lifetime of photocarriers. It increases with a decrease of ion energy. The N⁺GaAs devices exhibit ohmic dependence up to low voltage bias (< 10 V) and quadratic dependence at higher biases, however LT GaAs has linear dependence in the entire range of applied voltage biases [8]. During the implantation process it is very important to choose a right dose of ions of appropriate energy, which greatly influences penetration depth. Due to the above mentioned advantages, especially ultra-short carrier lifetime, N⁺GaAs material is very promising for the preparation of high-speed and broadband optoelectronics devices [9]: sensitive photodetectors [10], photoconductive switches [11] and photomixers for generation of pulses [12].

Conventional oscilloscopic characterization techniques for the measurement of fast response photodetectors are unsuitable in the THz region, due to the bandwidth limitation. Electro-optic sampling (EOS) overcomes some limitations and increases the bandwidth into the THz regions. The external EOS has been first constructed by Valdmanis et al. [13] and then frequently applied to measure temporal resolution of fast photodetectors [14], to characterise coplanar transmission lines and to detect electrical signals of THz frequency [15]. Typical EOS consists of a femtosecond pulsed laser, a photodetector (switch) for electrical pulse generation and an electro-optical crystal as a probe to detect the electric field. The amplitude and width of the generated electrical pulse strongly depend on numerous parameters: the optical pulse duration, the charge carrier lifetime, mobility and concentration, transit time between the electrodes, and the RC time constant of the transmission line circuit [16].

* corresponding author; e-mail: wierzba@if.pw.edu.pl

According to the theory of Sano and Shibata [17], the observation of a short pulse is possible for asymmetric excitation and zero distance propagation for switching and sampling spots, due to a highly nonuniform distribution of the electric field for finger configuration.

The aim of this paper is to demonstrate the electro-optic sampling system constructed for measurements of temporal responses of high-speed photodetectors based on N^+ -implanted GaAs compared with the same geometry MSM fabricated on LT GaAs. The structural difference of these materials was confirmed by X-ray diffraction and diffuse scattering analysis. Changes in structural parameters, such as crystal lattice constant, radius of nanoclusters and density of dislocations were observed after implantation.

2. Experimental

The investigated photodetectors were fabricated from 1.5 μm thick N^+ GaAs or LT GaAs layer grown in a commercial Varian Mod GEN II molecular beam epitaxy (MBE) on 500 μm thick GaAs substrates, separated by 0.15 μm of AlAs. Both photodetectors had a metal–semiconductor–metal structure (MSM) with the same geometry: finger width $l_w = 11 \mu\text{m}$ and spacing $l_a = 17 \mu\text{m}$ (see Fig. 1). Figure 2 presents the calculated influence of finger geometry on the capacity C of MSM [18]. With increasing l_a , the capacitance decreases. Calculated capacitance for the measured structure $C = 9.8 \text{ fF}$ and quantum efficiency $\eta = 30\%$. The interdigitated MSM Ti/Au finger contacts of 50/600 nm thickness were patterned on the top of the layer by conventional photolithography process. Dark current–voltage characteristics of N^+ GaAs and LT GaAs photodetectors, measured at room temperature, are presented in Fig. 3. N^+ GaAs detector exhibits ohmic I – U dependence up to bias voltage $U = 15 \text{ V}$. For higher biases I – U dependence becomes quadratic, due to the existence of free carriers from non-implanted region, where the conductivity is much higher. LT GaAs exhibits ohmic dependence and higher dark current in the entire range of bias voltage, because carrier concentration and mobility of LT GaAs are higher.

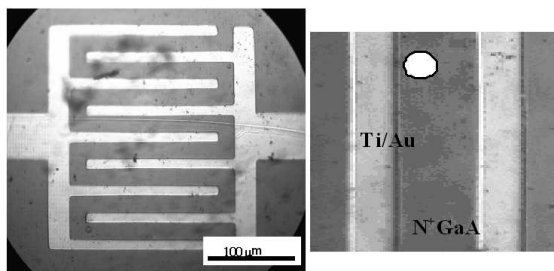


Fig. 1. Photograph of the investigated N^+ GaAs photodetector (left), investigated area with marked excitation spot position (right).

The response of N^+ GaAs photodetector was measured with an EOS system utilizing 80 fs wide optical pulses

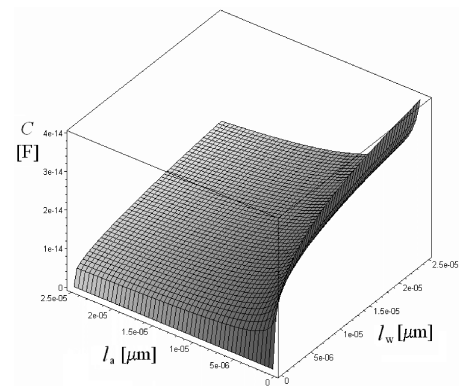


Fig. 2. MSM capacitance for various finger width l_w and finger spacing l_a .

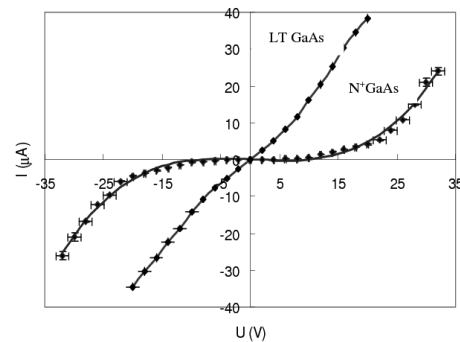


Fig. 3. I – U characteristics of N^+ GaAs and LT GaAs.

from a commercial Ti:sapphire laser (Tsunami, Spectra Physics) at 795 nm and 80 MHz repetition rate (see Fig. 4). The laser beam was split by a beam splitter 50/50 into two beams: a sampling (probe) and an exciting (pump) beam. The pump beam was directed through the LiTaO_3 crystal utilized as an external probe to detect the electro-optic signal. The photodetector response was analyzed by the time delayed probe beam, 45° polarized with respect to the optical axis of the electro-optical crystal, which caused total internal reflection at the bottom facet [19]. The change of polarization was decoded by a polarizing beam splitter. The difference in the electrical signals from two conventional photodiodes was collected by a lock-in amplifier. To obtain sub-picosecond response time probe and pump beams had to be carefully positioned on a layer of N^+ GaAs. Two conditions had to be fulfilled: asymmetric excitation and zero propagation distances. High resolution X-ray measurements were done on PANalytical's X'Pert PRO MPD diffractometer with vertical θ – 2θ goniometer.

3. Results

Figure 5 presents the photoresponse signal of N^+ GaAs photodetector. The transient exhibits 1.15 ps FWHM which corresponds to 400 GHz (3 dB bandwidth). Signal amplitude peak $\approx 1 \text{ mV}$ is higher than the amplitude

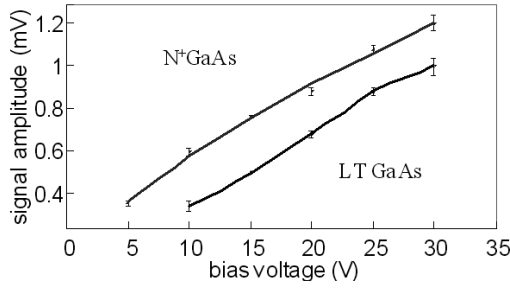


Fig. 9. Amplitude as a function of bias voltage.

not lead to any additional carrier generation. The saturation level for LT GaAs photodetector was reached earlier at 23 mV/W. Figure 9 presents changes in the signal amplitude with voltage. The obtained results indicate a linear $I-U$ dependence in the whole voltage range, similarly to LT GaAs. Similar dependences have been observed for other excitation power and bias voltage, too. However signal amplitudes are higher for N^+ GaAs.

To explain the difference between inside qualities of crystal structures for implanted and non-implanted photodetectors, high resolution X-ray diffractometry (HRXRD) and diffuse scattering analyses were utilized. Crystal lattice parameters were determined by $\lambda = (1.540593 \pm 0.000005) \text{ \AA}$ as Cu $K_{\alpha 1}$ [21]. Symmetrical reflex GaAs (004) was selected for measurements. For N^+ GaAs, $2\theta = (66.356 \pm 0.002)^\circ$ yields lattice constant $a = (5.6304 \pm 0.0003) \text{ \AA}$. For LT GaAs, $2\theta = (66.0798 \pm 0.002)^\circ$ yields $a = (5.651 \pm 0.0003) \text{ \AA}$. The second (smaller) peak corresponds to AlAs layer and for $2\theta = (66.4278 \pm 0.006)^\circ$, $a = (5.625 \pm 0.0009) \text{ \AA}$. From experimental results for both implanted (Fig. 12b) and non-implanted detector (Fig. 13b) we obtained $\text{FWHM}^{(004)} = 18''$. A small increase in diffuse scattering can be observed for N^+ GaAs sample: along Q_x direction $\text{FWHM}_{N^+GaAs}/\text{FWHM}_{LTGaAs}(Q_x) = 1.3$, along Q_z direction $\text{FWHM}_{N^+GaAs}/\text{FWHM}_{LTGaAs}(Q_z) = 1.7$. Utilizing calculations of Kaganer et al. [22] for 60° dislocation with the Burgers vector $1/2 \langle 110 \rangle$ we obtained the ratio of linear density of dislocations $\rho_{N^+GaAs}/\rho_{LTGaAs}(Q_x) = 1.6$, while $\rho_{N^+GaAs}/\rho_{LTGaAs}(Q_z) = 2.2$. For similar ratio of FWHM in direction Q_z the changes are insignificant. Symmetrization and normalization intensity process for measurements points (Fig. 12b and Fig. 13b) was performed according to [5] in the Huang region. It is presented in Fig. 12a and Fig. 13a as the graph of $I^s(q_0)/I_0$ as a function of $\ln(q_0)$. We obtained parameters for LT GaAs sample of line $I^s(q_0)/I_0 = -0.4923 \ln(q_0) - 3.890$, intercept fitted line with $I_h^s/I_0 = 0$ gives $R_0 = (445 \pm 10) \text{ nm}$, for N^+ GaAs $I^s(q_0)/I_0 = -0.400 \ln(q_0) - 3.119$, intercept gives $R_0 = (396 \pm 9) \text{ nm}$.

The radii of nanoclusters, and the FWHM width of the diffraction curve are comparable for both materials, therefore quantity and size of defects are similar in LT GaAs and N^+ GaAs. This is verified by the response times measured by EOS.

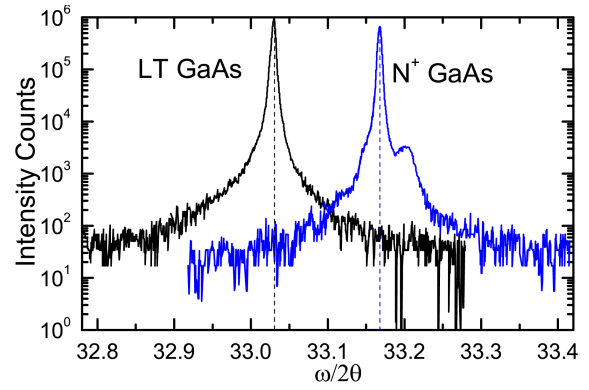


Fig. 10. Experimental diffraction curves GaAs(004) for LT GaAs (left curve) and N^+ GaAs (right curve).

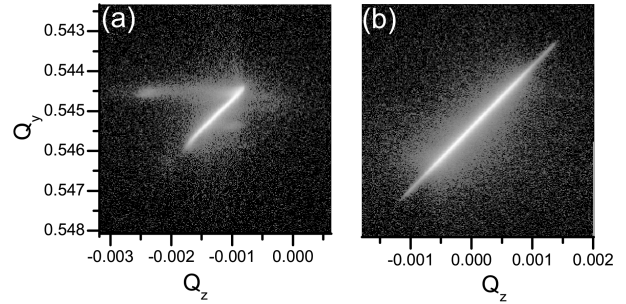


Fig. 11. Reciprocal space map GaAs(004) for N^+ GaAs detector (left) and LT GaAs (right).

4. Conclusions

The response time of N^+ GaAs photodetector $\approx 1.15 \text{ ps}$ FWHM corresponds to $\approx 400 \text{ GHz}$, 3 dB bandwidth. It is comparable to the response time of LT GaAs, due to the limitation of time constant τ by the MSM capacitance. It was independent of voltage biases and optical power used. The optimal signal is obtained by illuminating a small semiconductor area at the edge of the finger structure only, when both excitation and switching beams

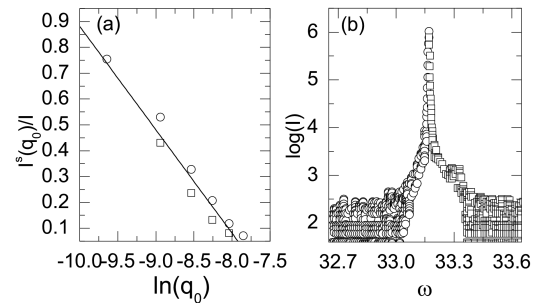


Fig. 12. (a) Symmetrical normalized intensity of diffuse scattering vs. function of $\ln(q_0)$. (b) Experimental rocking curves GaAs (004) for N^+ GaAs sample, used to diffuse scattering analyses.

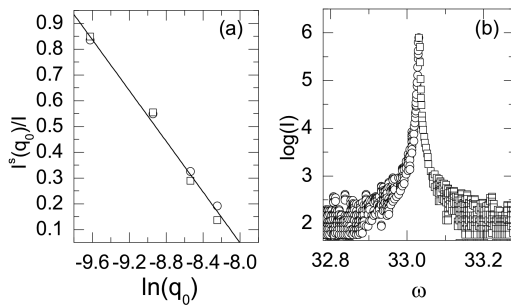


Fig. 13. (a) Symmetrical normalized intensity of diffuse scattering vs. function of $\ln(q_0)$. (b) Experimental rocking curves GaAs (004) for LT GaAs sample used to diffuse scattering analyses.

are positioned close to the positive electrode. A linear increase in the signal amplitude has been observed for moderate optical powers and for all biases used. X-ray diffractions and diffuse scattering analyses indicate that the implantation process changes structural parameters: increases diffuse scattering, decreases radii of nanoclusters and lattice constant. Nanoclusters radii and FWHM of rocking curves for both samples are similar, therefore the response time measured by EOS was almost comparable. The attributes presented in this paper suggest that the nitrogen-ion-implanted GaAs is a good alternative for LT GaAs as a material for fabrication of highly sensitive devices for optoelectronic high-speed applications.

Acknowledgments

We would like to thank Prof. Roman Sobolewski, from Department of Electrical and Computer Engineering, University of Rochester for stimulating discussions.

References

[1] M. Lambsdorff, J. Kuhl, J. Rosenzweig, A. Axmann, J. Schneider, *Appl. Phys. Lett.* **58**, 1881 (1991).
 [2] B. Breeger, E. Wendler, C. Schubert, W. Wesch, *Nucl. Instrum. Methods Phys. Res. B* **161-163**, 415 (2000).
 [3] A. Claverie, F. Namavar, Z. Liliental-Weber, *Appl. Phys. Lett.* **62**, 1271 (1993).

[4] A.I. Baranov, L.S. Smirnov. *Fiz. Tech. Poluprovodn.* **7**, 2227 (1973) (in Russian).
 [5] J.R. Patel, *J. Appl. Cryst.* **8**, 186 (1975).
 [6] M. Mikulics, M. Marso, I. Cãmara Mayorga, R. Güsten, S. Stanček, P. Kováč, S. Wu, Xia Li, M. Khafizov, R. Sobolewski, E.A. Michael, R. Schieder, M. Wolter, D. Buca, A. Förster, P. Kordoš, H. Lüth, *Appl. Phys. Lett.* **87**, 041106 (2005).
 [7] J.F. Chen, J.S. Wang, M.M. Huang, N.C. Chen, *Appl. Phys. Lett.* **76**, 2283 (2000).
 [8] M. Mikulics, M. Marso, P. Kordoš, S. Stanček, P. Kováč, X. Zheng, R. Sobolewski, *Appl. Phys. Lett.* **83**, no 1719 (2003).
 [9] E. Peytavit, S. Arscott, D. Lippens, G. Mouret, S. Matton, P. Masselin, R. Bocquet, J.F. Lampin, L. Desplanque, F. Mollot, *Appl. Phys. Lett.* **81**, 1174 (2002).
 [10] X. Zheng, R. Sobolewski, Y. Xu, R. Adam, M. Mikulics, M. Siegel, P. Kordoš, *Appl. Opt.* **42**, 1726 (2003).
 [11] G.A. Mourou, W. Knox, *Appl. Phys. Lett.* **35**, 492 (1979).
 [12] Y. Shen, P. Upadhyay, E. Linfield, H. Beere, A. Davies, *J. Appl. Phys.* **83**, 3117 (2003).
 [13] J. Valdmanis, G. Mourou, W. Gabel, *Appl. Phys. Lett.* **41**, 211 (1982).
 [14] S. Alexandrou, R. Sobolewski, T. Hsiang, *IEEE J. Quant. Electron.* **28**, 2325 (1992).
 [15] E. Harmon, M. Melloch, J. Woodall, D. Nolte, N. Otsuka, C. Chang, *Appl. Phys. Lett.* **63**, 2248 (1993).
 [16] J. Holzman, F. Vermeulen, A. Elezzabi, *IEEE J. Quant. Electron.* **36**, 130 (2000).
 [17] E. Sano, T. Shibata, *Appl. Phys. Lett.* **55**, 2748 (1989).
 [18] M. Ito, O. Wada, *IEEE J. Quant. Electron.* **QE-22**, no 7, (1986).
 [19] U. Keil, D. Dykaar, *Appl. Phys. Lett.* **61**, 1504 (1992).
 [20] R. Hofmann, H.J. Pfeleiderer, *Microelectron. Eng.* **31**, 377 (1996).
 [21] G. Hölzer, M. Fritsch, M. Deutsch, J. Härtwig, E. Förster, *Phys. Rev. A* **56**, 4554 (1997).
 [22] V. Kaganer, R. Kohler, M. Schmidbauer, R. Optiz, B. Jenichen, *Phys. Rev. B* **55**, 170 (1997).